JOURNAL OF CHEMICAL & ENGINEERING DATA

ARTICLE

pubs.acs.org/jced

Vapor−Liquid Equilibrium Measurements of Difluoromethane + [Emim]OTf, Difluoromethane + [Bmim]OTf, Difluoroethane + [Emim]OTf, and Difluoroethane + [Bmim]OTf Systems

Li Dong, Danxing Zheng,* Guangming Sun, and Xianghong Wu

College of Chemical Engineering, Beijing University of Chemical Technology, Beijing 100029, China

ABSTRACT: Solubility behaviors of binary difluoromethane (HFC-32) and 1,1-difluoroethane (HFC-152a) systems with ionic liquids (ILs) 1-ethyl-3-methylimidazolium trifluoromethanesulfonate ([Emim]OTf) and 1-butyl-3-methylimidazolium trifluoromethanesulfonate ([Bmim]OTf) have been studied by using an isothermal synthetic apparatus at temperatures (273.15, 298.15, 323.15 and 348.15) K and at pressures (0.04 to 1.0) MPa. Experimental solubility data were successfully correlated with the nonrandom two-liquid (NRTL) activity coefficient model. It was found that the solubility of hydrofluorocarbons (HFCs) in ILs is affected by the change of alkyl chain length in the cation.

INTRODUCTION

Energy resources have become a serious problem in current situations. To improve energy efficiency by the utilization of waste heat or extending the operating temperature range, compression/absorption hybrid cycles, which combine a vapor compression cycle with an absorption cycle, have been investigated to have good research and development prospects under such condition.[1]

Fluorinated refrigerants have been widely used in most vapor compression refrigeration cycles, because of their thermophysical properties.[2] The restrictions to the use of chlorofluorocarbons (CFCs) and hydrochlorofluorocarbons (HCFCs) as working fluids in heat pumps and refrigeration systems have led to the use of hydrofluorocarbons as alternatives.[3,4] They are demanded to be developed in a harmless way and accompanied by high capacity and high efficiency in many applications.[5]

On the other hand, for the absorption refrigeration cycles, during the past decade, growing attention has been given to ILs for their performance applied as alternative absorbent species of working fluids, i.e., NH_3-H_2O and $H_2O-LiBr$, to overcome existing problems and to improve the overall cycle efficiency.[6]

Selecting environmentally acceptable HFCs as refrigerants, combined with appropriate ILs, can be adopted as working pairs for compression/absorption hybrid cycles. They can be used in numerous applications, such as heat pumps, air conditioners, and low-temperature refrigeration.[7,8]

However, to use HFCs as working fluids, an absorbent that is compatible with HFCs needs to be found. Important factors for selection of a successful absorbent are dependent on the refrigerant solubility in the absorbent. The capacity of the HFCs solubility in ILs has a great impact on the refrigeration cycle performance. Research and development on efficient working pairs of novel ILs with high performance are hot topics.

Shiflett and Yokozeki[9] investigated the solubilities of six different HFCs, trifluoromethane (HFC-23), difluoromethane (HFC-32), pentafluoroethane (HFC-125), 1,1,1,2-tetrafluoroethane (HFC-134a), 1,1,1-trifluoroethane (HFC-143a), and 1,1-difluoroethane (HFC-152a), in two ILs [Bmim]PF_6 and [Bmim]BF_4, respectively, by using a gravimetric microbalance at various isothermal conditions. The results show that the solubilities for HFCs decrease have the following order: HFC-32 > HFC-152a > HFC-23 > HFC-134a > HFC-125 > HFC-143a. HFC-32 and HFC-152a have good prospects, shown by their solubilities in ILs. At the same time, both HFC-32 and HFC-152a have relatively short atmospheric lifetimes and advantages with lower values of ozone depletion potential and global warming potential.

Ren and Scurto,[10] Shiflett and collaborators,[11−16] Kumelan et al.,[17] Shariati and Peters[18] measured phase behavior and equilibria data for various HFCs with ILs. The ILs contain anions of tetrafluoroborate ([BF_4]), hexafluorophosphate ([PF_6]), bis(trifluoromethylsulfonyl)imide ([Tf_2N]), bis(pentafluoroethylsulfonyl)imide ([BEI]), acetate ([Ac]), thiocyanate ([SCN]), methyl sulfate ([$MeSO_4$]), and so on. The results show that HFCs solubility is greater in ILs with anions, such as [PF_6] and [Tf_2N], which consist of fluorinated groups. However, ILs containing [PF_6] anion are unstable and degrade rapidly.[19] Due to the high viscosity of the [PF_6] ILs,[20] the dissolution process takes a lot of time. The molecular weight of the [Tf_2N]-based ILs is big, and the cost of the ILs is very high.

In this study, HFC-32 and HFC-152a were adopted as environmentally-friendly refrigerants. ILs [Emim]OTf and [Bmim]OTf were chosen as the absorbents having good miscibility with the HFCs. The solubilities of HFC-32 and HFC-152a with [Emim]OTf and [Bmim]OTf were measured at temperatures between (273.15 and 348.15) K. The experimental data were fitted with the nonrandom two-liquid (NRTL) activity coefficient model.

MATERIAL AND METHODS

Materials. The hydrofluorocarbon HFC-32 (CH_2F_2, CAS registry no. 75-10-5) and HFC-152a (CH_3-CHF_2, CAS registry

Received: June 5, 2011
Accepted: August 3, 2011
Published: August 23, 2011

dx.doi.org/10.1021/je2005566 | J. Chem. Eng. Data 2011, 56, 3663–3668

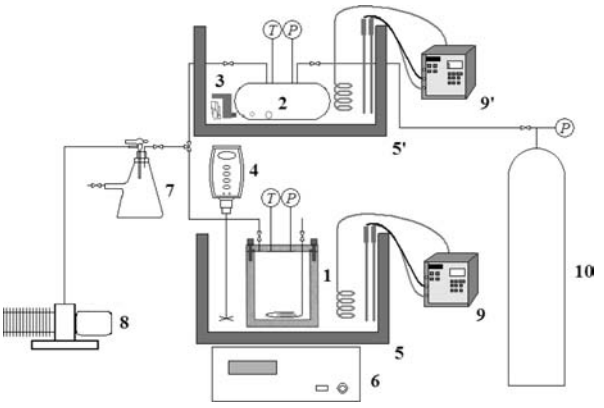

Figure 1. Schematic diagram of the isothermal synthetic apparatus of this work: 1, equilibrium cell; 2, gas chamber; 3, circulation pump; 4, overhead blender; 5, 5′, isothermal water bath; 6, magnetic stirrer; 7, buffer; 8, vacuum pump; 9, 9′, temperature controller; 10, gas storage.

no. 75-37-6) were obtained from Shandong Dongyue Fluorine & Silicon Material Co., Ltd. The purities of HFC-32 and HFC-152a are 99.97% and 99.98% in mass fraction, respectively.

IL [Emim]OTf ($C_7H_{11}F_3N_2O_3S$, CAS registry no. 145022-44-2) and [Bmim][OTf] ($C_9H_{15}F_3N_2O_3S$, CAS registry no. 174899-66-2) were purchased from Shanghai Chengjie Chemical Co., Ltd. The purities are better than 99% in mass fraction.

HFC-32 and HFC-152a were used without any further purification, but [Emim]OTf and [Bmim][OTf] were dried under reduced pressure thanks to a vacuum pump prior to use.

Measurement of Solubility. To investigate the vapor−liquid equilibrium behavior of the sample binary system, the gas solubility measurements were carried out in an isothermal synthetic apparatus similar to those employed by Fischer et al."[22] with a few modifications. The schematic diagram of the apparatus is shown in Figure 1. The apparatus mainly consists of a stainless steel equilibrium cell with constant volume (V_E, 321 mL), gas sampling system, temperature control system, and a vacuum system. An isothermal water bath is used to thermostat the equilibrium cell, and a magnetic stirrer is used to accelerate the equilibrium in the cell. The temperature stability of the equilibrium cell and the isothermal water bath is ±0.03 K by using a controller made by JULABO Labortechnik GmbH. The temperature of the gas chamber is measured with PT100 resistance thermometers (273.2 to 373.2 K) within an uncertainty of 0.1 K. The pressure of the equilibrium cell is measured with a PTX7533 pressure sensor (0 to 6 MPa) and the pressure of the gas chamber is measured by a PTX7517 pressure sensor (0 to 6 MPa). The sensors of PTX7533 and PTX7517 have the maximum errors of 0.025% full scope and 0.038% full scope, respectively, which were manufactured and calibrated by GE DRUCK. The mass of the ILs placed into the equilibrium cell was measured using a Mettler Toledo AL 204 balance with an uncertainty of 10^{-4} g.

The elements of the isothermal synthetic method are to load precisely known amounts of the pure components into a thermoregulated equilibrium cell and to measure the pressure as a function of composition in the system. At the beginning of each experimental run, (30 to 40) g of IL was loaded into the stainless steel equilibrium cell, and the mass of IL was precisely recorded (m_s). The equilibrium cell was sealed and evacuated by an oil pump to approximately 1 kPa. After the thermostated system has worked and reached a certain temperature, the temperature and pressure of the gas chamber were recorded (T_A, p_A). The gas chamber was filled directly from gas storage to a pressure greater than the pressure in the equilibrium cell. The gases were then filled into the equilibrium cell stepwise from the gas chamber. The total volume of the gas injection system and of the gas chamber was 1005 mL (V_g). With gases dissolving into the absorbent, the pressure and the temperature in the equilibrium cell varied, and after an absorption equilibrium process, they would stabilize at the equilibrium values. The temperatures and pressures of the gas chamber were recorded (T_B, p_B). The pressure and temperature of the cell were recorded when the equilibrium was reached (T, p). To ensure sufficient time for gas−liquid equilibrium, the IL samples were maintained at each pressure set point for (1 to 4) h.

The solubility data can be calculated with the temperature, pressure, and volume values obtained during the above procedure as follows.

$$x_1 = \frac{n_1}{n_1 + n_2} \tag{1}$$

where x_1 is the gas solubility (mole fraction), n_2 is the number of moles of IL calculated according to $n_2 = m_s/M_s$, M_s is the molar mass of IL (i.e., 260.24 and 288.29 for [Emim]OTf and [Bmim]OTf, respectively), and n_1 is the number of moles of gas absorbed in IL calculated from

$$n_1 = n_{1,in} - n_1^v = (n_B - n_A) - n_1^v \tag{2}$$

where $n_{1,in}$ is the amount of gas injected into the equilibrium cell and n_B and n_A are the amounts of gas in the gas chamber before and after injection, which can be calculated using suitable equations of state from the (T_B, p_B, V_g) and (T_A, p_A, V_g) data. The equation of state used in the NIST REFPROP[23] computer program was used in this work. n_1^v is the amount of gas injected into the equilibrium cell but not dissolved in IL, because IL has negligible vapor pressure; n_1^v can be calculated using REFPROP from the (T, p, V_v) data. Assuming neglect of the volume change of gas-dissolved IL, V_v can be given as $V_v = V_E/V_2$, where the volume V_2 of IL in the cell is calculated from its mass and density.[24,25]

In the above-described process, the temperature, pressure, IL loading, and volume are measured, but the composition has to be determined by evaluation of the raw data. The uncertainties of each experimental quantity are estimated as follows: pressure of the equilibrium cell 0.001 MPa, pressure of the gas chamber 0.0015 MPa, volume of the equilibrium cell 0.2%, volume of the gas chamber 0.2%, mass of solvent 10^{-4} g, temperature in the equilibrium cell 30 mK, temperature in the gas chamber 0.1 K. The uncertainties in solubility are estimated as follows.

$$\begin{aligned} x_1 &= \frac{n_1}{n_1 + n_2} = \frac{n_{1,in} - n_1^v}{n_{1,in} - n_1^v + n_2} \\ n_1^v &= \rho_1^v(T,p)\cdot V_v = \rho_1^v(T,p)\cdot(V_E - V_2) \\ x_1 &= \frac{n_1}{n_1 + n_2} = \frac{n_{1,in} - \rho_1^v(T,p)\cdot(V_E - V_2)}{n_{1,in} - \rho_1^v(T,p)\cdot(V_E - V_2) + n_2} \\ x_1 &= f(n_{1,in}, \rho_1^v, V_E, V_2) \end{aligned} \tag{3}$$

For an initial analysis, assume no errors in ($n_{1,in}$, ρ_1^v, V_E), i.e., only error in the solubility data arising from volume

Table 1. Comparison of Measured Solubilities for CO_2/Ethanol System at 313.15 K with Literature Values

literature	p/MPa	$x_{1,exp}$	$x_{1,lit}$	$\lvert x_{1,exp} - x_{1,lit}\rvert / x_{1,lit}$ (%)
Suzuki[26]	0.514	0.027	0.026	3.8
	1.155	0.063	0.064	1.6
	2.061	0.113	0.111	1.8
	3.020	0.167	0.166	0.6
Tsivintzelis[27]	1.600	0.088	0.088	0.0
	2.120	0.117	0.116	0.9
	3.270	0.181	0.183	1.1
	3.810	0.212	0.214	0.9

change.

$$x_1 = f(V_2)$$
$$(\delta x_1)^2 = \left(\frac{\partial x_1}{\partial V_2}\right)^2 (\delta V_2)^2$$
$$\left(\frac{\partial x_1}{\partial V_2}\right) = \frac{\rho_1^v n_2}{(n_{1,in} - \rho_1^v V_E + \rho_1^v V_2 + n_2)^2}$$
$$\left(\frac{\partial x_1}{\partial V_2}\right)^2 (\delta V_2)^2 = \left[\frac{\rho_1^v n_2}{(n_{1,in} - \rho_1^v V_E + \rho_1^v V_2 + n_2)^2}\right]^2 (\delta V_2)^2 \quad (4)$$

where δx_1 is the uncertainty in solubility and ρ_1^v is the gas molar density at the system T and p, which can be calculated by REFPROP program.[23] Assume that the volume expansion with refrigerant gases and ILs can reach 100% of the gas-free value.

Similarly, the errors in the other measurable are estimated as follows.

$$\left(\frac{\partial x_1}{\partial n_{1,in}}\right)^2 (\delta n_{1,in})^2 = \left[\frac{n_2}{(n_{1,in} - \rho_1^v V_E + \rho_1^v V_2 + n_2)^2}\right]^2 (\delta n_{1,in})^2$$
$$\left(\frac{\partial x_1}{\partial V_E}\right)^2 (\delta V_E)^2 = \left[\frac{n_2 \rho_1^v}{(n_{1,in} - \rho_1^v V_E + \rho_1^v V_2 + n_2)^2}\right]^2 (\delta V_E)^2$$
$$\left(\frac{\partial x_1}{\partial \rho_1^v}\right)^2 (\delta \rho_1^v)^2 = \left[\frac{n_2 (V_2 - V_E)}{(n_{1,in} - \rho_1^v V_E + \rho_1^v V_2 + n_2)^2}\right]^2 (\delta \rho_1^v)^2 \quad (5)$$

The overall uncertainties in solubility measurements are calculated by

$$x_1 = f(V_2, n_{1,in}, \rho_1^v, V_E)$$
$$\delta x_1 = \left[\left(\frac{\partial x_1}{\partial V_2}\right)^2 (\delta V_2)^2 + \left(\frac{\partial x_1}{\partial n_{1,in}}\right)^2 (\delta n_{1,in})^2 + \left(\frac{\partial x_1}{\partial \rho_1^v}\right)^2 (\delta \rho_1^v)^2 + \left(\frac{\partial x_1}{\partial V_E}\right)^2 (\delta V_E)^2\right]^{1/2} \quad (6)$$

The estimated uncertainty for each data point was listed in the data tables.

Apparatus Reliability Validation. To check the reliability of the experimental apparatus used in this work, the CO_2 solubilities in ethanol at 313.15 K were measured. The results are compared to those obtained by Suzuki et al.[26] and of Tsivintzelis et al.[27] for the CO_2/ethanol system at 313.15 K and reported in Table 1. The subscripts "exp" and "lit." of x_1 denote the experimental and literature mole fraction of CO_2, respectively. The calibration experiments indicated the maximum absolute relative deviation are respectively 3.8% for Suzuki et al. and 1.1% for Tsivintzelis et al., and the average absolute relative deviations are correspondingly 2.0% and 0.7%. It is shown that the data measured in this work are in good agreement with literature data, which indicates that the experimental apparatus is reliable and applicable.

Table 2. Experimental Solubility (T, p, x) Data of HFC-32 in [Emim]OTf

T/K	p/MPa	x_1	δx_1	T/K	p/MPa	x_1	δx_1
273.21	0.101	0.123	0.006	298.16	0.799	0.407	0.023
273.14	0.195	0.204	0.010	298.11	0.857	0.432	0.023
273.15	0.297	0.285	0.013	323.13	0.097	0.039	0.006
273.16	0.399	0.369	0.014	323.20	0.195	0.073	0.012
273.16	0.494	0.446	0.013	323.20	0.303	0.109	0.017
273.19	0.590	0.531	0.011	323.16	0.399	0.135	0.022
273.16	0.692	0.630	0.008	323.14	0.501	0.171	0.025
298.16	0.102	0.061	0.007	323.17	0.598	0.197	0.029
298.14	0.204	0.116	0.012	348.14	0.107	0.029	0.006
298.14	0.305	0.174	0.016	348.16	0.209	0.052	0.012
298.15	0.397	0.224	0.019	348.16	0.311	0.075	0.018
298.12	0.505	0.274	0.021	348.15	0.408	0.096	0.023
298.16	0.603	0.321	0.022	348.15	0.510	0.114	0.027
298.15	0.698	0.363	0.023				

Table 3. Experimental Solubility (T, p, x) Data of HFC-32 in [Bmim]OTf

T/K	p/MPa	x_1	δx_1	T/K	p/MPa	x_1	δx_1
273.19	0.104	0.140	0.007	298.15	0.723	0.434	0.022
273.15	0.195	0.243	0.011	298.17	0.830	0.484	0.022
273.19	0.303	0.358	0.012	298.13	0.902	0.521	0.021
273.13	0.412	0.465	0.012	323.22	0.101	0.047	0.007
273.17	0.500	0.547	0.010	323.16	0.205	0.083	0.014
273.17	0.593	0.639	0.008	323.13	0.299	0.117	0.020
273.14	0.636	0.683	0.007	323.12	0.400	0.150	0.025
298.12	0.098	0.069	0.007	323.15	0.507	0.191	0.029
298.16	0.200	0.139	0.013	348.12	0.103	0.033	0.007
298.12	0.301	0.200	0.017	348.20	0.201	0.065	0.014
298.14	0.400	0.264	0.020	348.23	0.299	0.090	0.019
298.16	0.530	0.333	0.022	348.24	0.403	0.114	0.025
298.19	0.623	0.384	0.022	348.15	0.500	0.137	0.029

RESULTS AND DISCUSSION

The measurements were performed at temperatures (273.15, 298.15, 323.15, and 348.15) K and at pressures from (0.04 to 1.0) MPa. The corresponding solubility results are given in Tables 2−5.

For an N-component system, the γ/Φ formulation of vapor/liquid equilibrium can be described by eq 7.[28]

$$y_i \Phi_i p = x_i \gamma_i p_i^s \qquad (i = 1, 2, \ldots, N) \quad (7)$$

where p is the system pressure, p_i^s expresses the saturated vapor pressure for the ith species, y_i, x_i, and γ_i are the vapor phase mole

dx.doi.org/10.1021/je2005566 |J. Chem. Eng. Data 2011, 56, 3663–3668

Table 4. Experimental Solubility (T, p, x) Data of HFC-152a in [Emim]OTf

T/K	p/MPa	x_1	δx_1	T/K	p/MPa	x_1	δx_1
273.22	0.040	0.049	0.003	323.14	0.368	0.226	0.016
273.24	0.074	0.108	0.005	323.16	0.447	0.282	0.017
273.25	0.157	0.269	0.007	323.20	0.528	0.332	0.018
273.16	0.198	0.376	0.006	323.14	0.756	0.473	0.017
298.15	0.096	0.066	0.006	348.15	0.111	0.048	0.006
298.15	0.173	0.135	0.010	348.14	0.204	0.088	0.011
298.15	0.279	0.255	0.012	348.17	0.308	0.140	0.015
298.14	0.386	0.369	0.012	348.17	0.423	0.202	0.019
298.15	0.454	0.452	0.011	348.16	0.519	0.259	0.020
323.14	0.116	0.061	0.007	348.16	0.645	0.325	0.021
323.13	0.240	0.143	0.013	348.16	0.741	0.371	0.021
323.15	0.314	0.194	0.015	348.16	0.848	0.429	0.020

Table 5. Experimental Solubility (T, p, x) Data of HFC-152a in [Bmim]OTf

T/K	p/MPa	x_1	δx_1	T/K	p/MPa	x_1	δx_1
273.22	0.056	0.095	0.004	323.15	0.500	0.350	0.019
273.23	0.097	0.184	0.006	323.16	0.619	0.426	0.019
273.24	0.144	0.302	0.007	323.15	0.734	0.494	0.018
273.24	0.191	0.409	0.006	323.16	0.813	0.536	0.017
298.14	0.117	0.121	0.008	348.13	0.107	0.060	0.007
298.13	0.218	0.222	0.012	348.15	0.223	0.123	0.013
298.18	0.290	0.306	0.013	348.15	0.313	0.178	0.017
298.16	0.371	0.386	0.013	348.15	0.414	0.230	0.020
298.16	0.460	0.496	0.011	348.18	0.513	0.291	0.021
323.15	0.105	0.078	0.007	348.12	0.641	0.352	0.023
323.15	0.248	0.182	0.014	348.13	0.743	0.399	0.023
323.15	0.421	0.305	0.018	348.13	0.879	0.470	0.021

fraction, the liquid phase mole fraction, and the activity coefficient for the ith species, respectively, and Φ_i donates the correction factor for the ith species, which can be calculated by

$$\Phi_i \equiv \frac{\hat{\phi}_i}{\phi_i^s}\exp\left[-\frac{v_i^L(p-p_i^s)}{RT}\right] = \exp\left[\frac{(B_i - v_i^L)(p-p_i^s)}{RT}\right] \quad (8)$$

where $\hat{\phi}_i$ is the vapor phase fugacity coefficient for the ith species, ϕ_i^s is the fugacity coefficient for the pure ith species as saturated vapor, B_i is the second virial coefficient for the ith species at the system temperature T, and R is the universal gas constant.

For the gas(1) + IL (2) binary system, because the concentration of the IL in the vapor phase can be neglected, eq 7 can be written as eq 9.

$$\gamma_1 = \frac{p\Phi_1}{x_1 p_1^s} = \frac{p\exp\left[\frac{(B_1 - v_1^L)(p-p_1^s)}{RT}\right]}{x_1 p_1^s} \quad (9)$$

where B_1, ${v_1}^L$, and ${p_1}^s$ can be obtained by REFPROP program.

Table 6. Parameters for the NRTL Model in This Work

system (1) + (2)	α	${\tau_{12}}^{(0)}$	${\tau_{12}}^{(1)}$ /K	${\tau_{21}}^{(0)}$	${\tau_{21}}^{(1)}$ /K	Δp/ MPa
HFC-32 + [Emim]OTf	0.240	−0.320	1259.4	−0.912	−145.71	0.014
HFC-32 + [Bmim]OTf	0.212	−3.258	1889.4	0.123	−515.76	0.010
HFC-152a + [Emim]OTf	0.538	−7.636	2894.0	−3.192	1057.7	0.014
HFC-152a + [Bmim]OTf	0.508	−6.760	2903.7	−4.657	1384.9	0.011

To correlate solubility data, several activity coefficient models such as Margules, Wilson, and NRTL models were used in previous work. For IL-containing systems the solubility data can be well represented by NRTL models.[9,11−16] The NRTL equation, containing five parameters for a binary system, is

$$\ln\gamma_1 = {x_2}^2\left[\tau_{21}\left(\frac{G_{21}}{x_1 + x_2 G_{21}}\right)^2 + \frac{G_{12}\tau_{12}}{(x_2 + x_1 G_{12})^2}\right] \quad (10)$$

$$\ln\gamma_2 = {x_1}^2\left[\tau_{12}\left(\frac{G_{12}}{x_2 + x_1 G_{12}}\right)^2 + \frac{G_{21}\tau_{21}}{(x_1 + x_2 G_{21})^2}\right] \quad (11)$$

where

$$G_{12} = \exp(-\alpha\tau_{12}) \qquad G_{21} = \exp(-\alpha\tau_{21}) \quad (12)$$

and

$$\tau_{12} = \tau_{12}^{(0)} + \tau_{12}^{(1)}/T \qquad \tau_{21} = \tau_{21}^{(0)} + \tau_{21}^{(1)}/T \quad (13)$$

The parameters α, $\tau_{12}^{(0)}$, $\tau_{12}^{(1)}$, $\tau_{21}^{(0)}$, and $\tau_{21}^{(1)}$ in eqs 12 and 13 were fitted to the experimental data by regression, performed with the least-squares method. These parameters are listed in Table 4 for the four systems. The result of the parameter estimation may be expressed as a deviation of the calculated and experimental pressures for each system. The average deviation Δp is calculated with

$$\Delta p = \sum_{i=1}^{N_p} |p_{cal,i} - p_{exp,i}|/N_p \quad (14)$$

where p_{cal} is the calculated pressure, p_{exp} is the experimental pressure, and N_p is the number of experimental points. The average deviations are also listed in Table 6.

Isothermal $p-x$ diagrams calculated with these parameters of the four systems are compared with experimental values in Figures 2−5, and the relative deviations $(p_{cal} - p_{exp})/p_{exp}$ between the experimental and calculated pressure are shown in Figure 6. It is shown that the relative deviations are within ±0.1, and the measurement deviations are higher at high mole fraction than at low mole fraction. But, generally speaking, the solubility data over the entire range of experimentally investigated temperature and pressure have been well-correlated using the NRTL model.

Within the temperature and pressure regions studied in this work, the solubility pressure monotonously increases with increasing gas mole fraction at a fixed temperature. The solubilities of HFC-32 and HFC-152a in [Emim]OTf and [Bmim]OTf decrease with rising temperature. The solubility behaviors of

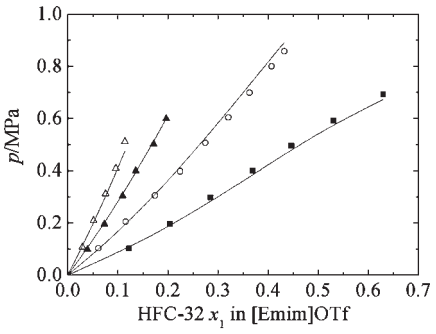

Figure 2. Isothermal $p-x$ diagram for HFC-32 + [Emim]OTf: ■, 273.15 K; ○, 298.15 K; ▲, 323.15 K; Δ, 348.15 K. Lines: NRTL model calculations. Symbols: present experimental data.

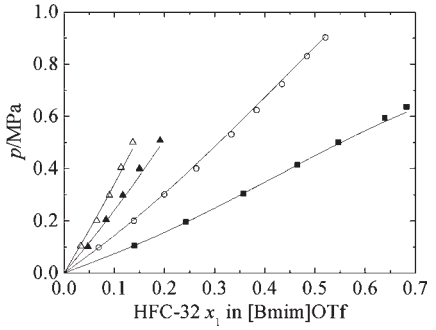

Figure 3. Isothermal $p-x$ diagram for HFC-32 + [Bmim]OTf: ■, 273.15 K; ○, 298.15 K; ▲, 323.15 K; Δ, 348.15 K. Lines: NRTL model calculations. Symbols: present experimental data.

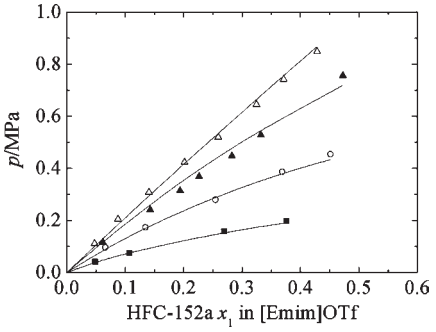

Figure 4. Isothermal $p-x$ diagram for HFC-152a + [Emim]OTf: ■, 273.15 K; ○, 298.15 K; ▲, 323.15 K; Δ, 348.15 K. Lines: NRTL model calculations. Symbols: present experimental data.

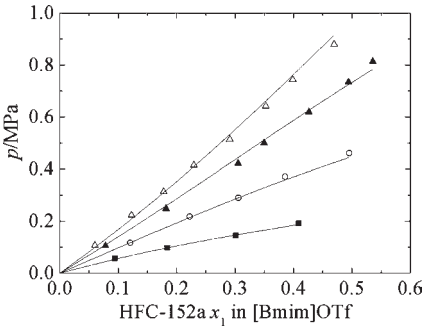

Figure 5. Isothermal $p-x$ diagram for HFC-152a + [Bmim]OTf: ■, 273.15 K; ○, 298.15 K; ▲, 323.15 K; Δ, 348.15 K. Lines: NRTL model calculations. Symbols: present experimental data.

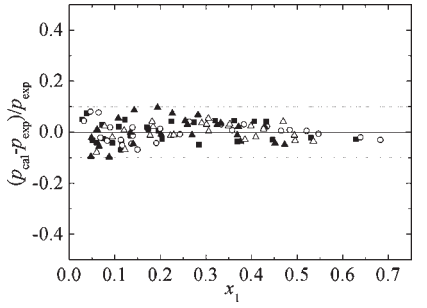

Figure 6. Relative deviation $(p_{cal} - p_{exp})/p_{exp}$ between the experimental and calculated pressure for HFC-IL binary mixtures: ■, HFC-32 + [Emim]OTf; ○, HFC-32 + [Bmim]OTf; ▲, HFC-152a + [Emim]OTf; Δ, HFC-152a + [Bmim]OTf.

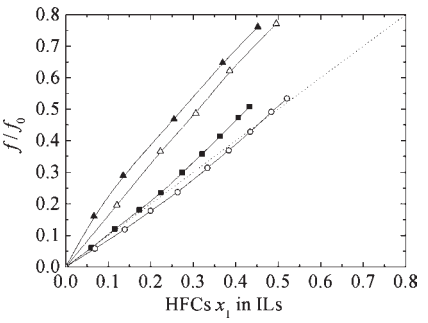

Figure 7. Normalized fugacity versus mole fraction for HFCs + ILs at 298.15 K: ■, HFC-32 + [Emim]OTf; ○, HFC-32 + [Bmim]OTf; ▲, HFC-152a + [Emim]OTf; Δ, HFC-152a + [Bmim]OTf. Solid lines: trend lines. Dashed line: Raoult's law. Symbols: present experimental data.

HFC-IL binary systems can be adjusted to meet the needs of applications by changing the pressure or temperature.

Aki et al.[29] reported that CO_2 solubility increased when the alkyl chain length was increased for imidazolium-based ILs with different anions at all pressures, and the increasing was more apparent at higher pressures. Extended to HFCs, for the four binary systems investigated in this work, the result is in accordance with the prior reports.[29] In the case where the [OTf] anion remains the same, the solubilities of both HFC-32 and HFC-152a in [Bmim]OTf are larger than those in [Emim]OTf. However, for the solubilities of different HFCs in the same IL, due to the differences in saturation vapor pressure of HFCs, the solubilities were compared using normalized pressure (or normalized fugacity).[9,30] The normalized fugacity was given by vapor phase fugacity of the solute, f, divided by the saturation fugacity, f_0. Figure 7 is a plot of the normalized fugacity of HFC-32 and HFC-152a versus mole fraction in [Emim]OTf and [Bmim]OTf at 298.15 K. It can be seen that when comparing HFC-32 with HFC-152a at the same f/f_0 ratio the solubility of HFC-32 is larger than that of HFC-152a. The results show that the combinations of fluorinated sulfonate anions ILs and environmentally-friendly refrigerants (HFC-32 and HFC-152a) are promising alternative

dx.doi.org/10.1021/je2005566 |J. Chem. Eng. Data 2011, 56, 3663–3668

working fluids of compression/absorption hybrid cycles for further research.

CONCLUSIONS

The solubility data of four binary systems HFC-32 + [Emim]OTf, HFC-32 + [Bmim]OTf, HFC-152a + [Emim]OTf, and HFC-152a + [Bmim]OTf were measured by means of an isothermal synthetic apparatus, at temperatures (273.15 to 348.15) K and pressures (0.04 to 1.0) MPa, respectively. The NRTL model was selected to correlate the experimental data. For HFC-32 + [Emim]OTf, HFC-32 + [Bmim]OTf, HFC-152a + [Emim]OTf, and HFC-152a + [Bmim]OTf systems, the average deviations in the pressure between experimental and calculated values are (0.014, 0.010, 0.014, and 0.011) MPa, respectively.

The results indicate that the solubility of HFC-32 is larger than that of HFC-152a for the same IL, and the solubility in [Bmim]OTf is larger than that in [Emim]OTf for the same HFC. Structural variations such as changing the length of the alkyl chain in the cation have a significant impact on the solubility of HFCs in ILs. The mixtures of HFC-32/HFC-152a and IL may be potential working fluids to improve the performances of compression/absorption hybrid cycles.

AUTHOR INFORMATION

Corresponding Author

*Tel. and Fax: +86-10-6441-6406. E-mail: dxzh@mail.buct.edu.cn..

ACKNOWLEDGMENT

The supports provided by the National Natural Science Foundation of China (No. 50890184) and the National Basic Research Program of China (No. 2010CB227304) for the completion of the present work are gratefully acknowledged.

REFERENCES

(1) Fukuta, M.; Yanagisawa, T.; Iwata, H.; Tada, K. Performance of compression/absorption hybrid refrigeration cycle with propane/mineral oil combination. *Int. J. Refrig.* **2002**, *25*, 907–915.

(2) Srikhirin, P.; Aphornratana, S.; Chungpaibulpatana, S. A review of absorption refrigeration technologies. *Renew. Sust. Energ. Rev.* **2001**, *5*, 343–372.

(3) Wahlstrom, A.; Vamling, L. Development of models for prediction of solubility for HFC working fluids in pentaerythritol ester compressor oils. *Int. J. Refrig.* **2000**, *23*, 597–608.

(4) Wahlstrom, A.; Vamling, L. Solubility of HFC32, HFC125, HFC134a, HFC143a, and HFC152a in a pentaerythritol tetrapentanoate ester. *J. Chem. Eng. Data* **1999**, *44*, 823–828.

(5) Fu, Y. D.; Han, L. Z.; Zhu, M. S. *PVT* properties, vapor pressures and critical parameters of HFC-32. *Fluid Phase Equilib.* **1995**, *111*, 273–286.

(6) Seiler, M.; Schwab, P.; Ziegler, F. Sorption systems using ionic liquid. *Proceedings of International Sorption Heat Pump Conference;* SAREK: Seoul, Korea, 2008; AB-040.

(7) Shiflett, M. B.; Yokozeki, A. Hybrid vapor compression-absorption cycle. WO 2006/124776 A2, 2006.

(8) Shiflett, M. B.; Yokozeki, A. Absorption cycle utilizing ionic liquid as working fluid. WO 2006/084262 A1, 2006.

(9) Shiflett, M. B.; Yokozeki, A. Solubility and diffusivity of hydrofluorocarbons in room-temperature ionic liquids. *AIChE J.* **2006**, *52*, 1205–1219.

(10) Ren, W.; Scurto, A. M. Phase equilibria of imidazolium ionic liquids and the refrigerant gas, 1,1,1,2-tetrafluoroethane (R-134a). *Fluid Phase Equilib.* **2009**, *286*, 1–7.

(11) Shiflett, M. B.; Harmer, M. A.; Junk, C. P.; Yokozeki, A. Solubility and diffusivity of difluoromethane in room-temperature ionic liquids. *J. Chem. Eng. Data* **2006**, *51*, 483–495.

(12) Shiflett, M. B.; Yokozeki, A. Solubility differences of halocarbon isomers in ionic liquid [emim][Tf2N]. *J. Chem. Eng. Data* **2007**, *52*, 2007–2015.

(13) Shiflett, M. B.; Harmer, M. A.; Junk, C. P.; Yokozeki, A. Solubility and diffusivity of 1,1,1,2-tetrafluoroethane in room-temperature ionic liquids. *Fluid Phase Equilib.* **2006**, *242*, 220–232.

(14) Shiflett, M. B.; Yokozeki, A. Binary vapor-liquid and vapor-liquid-liquid equilibria of hydrofluorocarbons (HFC-125 and HFC-143a) and hydrofluoroethers (HFE-125 and HFE-143a) with ionic liquid [emim][Tf2N]. *J. Chem. Eng. Data* **2008**, *53*, 492–497.

(15) Yokozeki, A.; Shiflett, M. B. Global phase behaviors of trifluoromethane in ionic liquid [bmim][PF6]. *AIChE J.* **2006**, *52*, 3952–3957.

(16) Shiflett, M. B.; Yokozeki, A. Gaseous absorption of fluoromethane, fluoroethane, and 1,1,2,2-tetrafluoroethane in 1-butyl-3-methylimidazolium hexafluorophosphate. *Ind. Eng. Chem. Res.* **2006**, *45*, 6375–6382.

(17) Kumełan, J.; Kamps, A. P.; Tuma, D.; Yokozeki, A.; Shiflett, M. B.; Maurer, G. Solubility of tetrafluoromethane in the ionic liquid [hmim][Tf2N]. *J. Phys. Chem. B* **2008**, *112*, 3040–3047.

(18) Shariati, A.; Peters, C. J. High-pressure phase behavior of systems with ionic liquids: measurements and modeling of the binary system fluoroform + 1-ethyl-3-methylimidazolium hexafluorophosphate. *J. Supercrit. Fluids* **2003**, *25*, 109–117.

(19) Aki, S. N.; Mellein, B. R.; Saurer, E. M.; Brennecke, J. F. High-pressure phase behavior of carbon dioxide with imidazolium-based ionic liquids. *J. Phys. Chem. B* **2004**, *108*, 20355–20365.

(20) Kenneth, R. H.; Lawrence, A. W.; Mitsuhiro, K. Temperature and pressure dependence of the viscosity of the ionic liquid 1-butyl-3-methylimidazolium hexafluorophosphate. *J. Chem. Eng. Data* **2005**, *50*, 1777–1782.

(21) Fischer, K.; Gmehling, J. J. $P-x$ and γ^{∞} data for the different binary butanol-water systems at 50 °C. *J. Chem. Eng. Data* **1994**, *39*, 309–314.

(22) Fischer, K.; Wilken, M. Experimental determination of oxygen and nitrogen solubility in organic solvents up to 10 MPa at temperatures between 298 and 398 K. *J. Chem. Thermodyn.* **2001**, *33*, 1285–1308.

(23) Lemmon, E. W.; Huber, M. L.; McLinden, M. O. *A computer program, REFPROP*, Version 8.0; National Institute of Standards and Technology: Gaithersburg, MD, 2005.

(24) Rodriguez, H.; Brennecke, J. F. Temperature and composition dependence of the density and viscosity of binary mixtures of water + ionic liquid. *J. Chem. Eng. Data* **2006**, *51*, 2145–2155.

(25) Soriano, A. N.; Doma, B. T.; Li, M. H. Measurements of the density and refractive index for 1-n-butyl-3-methylimidazolium-based ionic liquids. *J. Chem. Thermodyn.* **2009**, *41*, 301–307.

(26) Suzuki, K.; Sue, H.; Itou, M.; Smith, R. L.; Inomata, H.; Arai, K.; Saito, S. Isothermal vapor-liquid equilibrium data for binary systems at high pressures: carbon dioxide-methanol, carbon dioxide-ethanol, carbon dioxide-1-propanol, methane-ethanol, methane-1-propanol, ethane-ethanol, and ethane-1-propanol systems. *J. Chem. Eng. Data* **1990**, *35*, 63–66.

(27) Tsivintzelis, I.; Missopolinou, D.; Kalogiannis, K.; Panayiotou, C. Phase compositions and saturated densities for the binary systems of carbon dioxide with ethanol and dichloromethane. *Fluid Phase Equilib.* **2004**, *224*, 89–96.

(28) Smith, J. M.; Van Ness, H. C.; Abbott, M. M. *Introduction to Chemical Engineering Thermodynamics*, 6th ed.; McGraw-Hill: New York, 2002.

(29) Aki, S. N.; Mellein, B. R.; Saurer, E. M.; Brennecke, J. F. High-pressure phase behavior of carbon dioxide with imidazolium-based ionic liquids. *J. Phys. Chem. B* **2004**, *108*, 20355–20365.

(30) Shiflett, M. B.; Yokozeki, A. Separation of difluoromethane and pentafluoroethane by extractive distillation using ionic liquid. *Chem. Today* **2006**, *24*, 28–30.